

ARTICLE OPEN



Multilevel brain functional connectivity and task-based representations explaining heterogeneity in major depressive disorder

Qi Liu^{1,9}, Xinqi Zhou^{2,9}, Chunmei Lan³, Xiaolei Xu⁴, Yuanshu Chen², Taolin Chen⁵, Jinhui Wang⁶, Bo Zhou¹, Dezhong Yao⁷, Keith M. Kendrick⁷, Benjamin Becker^{8,10} and Weihua Zhao^{1,7,10}

© The Author(s) 2025

Major depressive disorder (MDD) is a devastating mental disorder characterized by considerable clinical and biological heterogeneity. While comparable clinical symptoms may represent a common pathological endpoint, it is conceivable that distinct neurophysiological mechanisms underlie their manifestation. In this study, both static and model-based dynamic functional connectivity were employed as predictive variables in the normative model to map multilevel functional developmental trajectories and determined clusters of distinguishable MDD subgroups in a large multi-site resting fMRI dataset of 2428 participants (healthy controls: $N = 1128$; MDD: $N = 1300$). An independent cohort of 72 participants (healthy controls: $N = 35$; MDD: $N = 37$) with both resting fMRI and task-based fMRI data was utilized to validate the identified MDD subtypes and explore subtype-specific task-based neural representations. Our findings indicated brain-wide, interpatient heterogeneous multilevel brain functional deviations in MDD. We identified two distinct and reproducible MDD subtypes, exhibiting comparable severity of clinical symptoms but opposing patterns of multilevel functional deviations. Specifically, MDD subtype 1 displayed positive deviations in the frontoparietal and default mode networks, coupled with negative deviations in the occipital and sensorimotor networks. Conversely, MDD subtype 2 exhibited a significantly contrasting deviation pattern. Additionally, we found that these two identified MDD subtypes exhibited different neural representations during empathic processing, while the subtypes did not differ during implicit face processing. These findings underscore the neurobiological complexity of MDD and highlights the need for a multifaceted approach to diagnosis and treatment that can be tailored specifically to individual subtypes, facilitating personalized and more effective interventions for individuals with MDD.

Translational Psychiatry (2025)15:199; <https://doi.org/10.1038/s41398-025-03413-4>

INTRODUCTION

Major depressive disorder (MDD) is a highly prevalent and burdensome mental disorder, with its onset commonly occurring during adolescence and high rates of chronification in later life leading to a tremendous burden of disease [1–3]. Those afflicted with MDD typically exhibit a range of clinical symptoms, including depressive mood and anhedonia as well as cognitive impairment, somatic symptoms, social deficits and recurrent suicidal thoughts [4–7]. According to the most recent Diagnostic and statistical manual of mental disorders (DSM-5) [8], a diagnosis of MDD with the same severity can encompass a vast array of symptom combinations. Together with variations in the specific symptoms, variations in the age of onset, duration of illness, presence of comorbid mental or neurological disorders and environmental

factors can collectively result in the physiological heterogeneity among individuals diagnosed with MDD. This heterogeneity poses a significant challenge in developing effective diagnostic and treatment strategies. Therefore, a more nuanced and individualized approach is imperative in understanding and treating MDD.

During recent decades, researchers have sought to identify MDD subtypes relying on clinical symptoms, genetics and other neurobiological features [9–11]. A growing number of studies have employed neuroimaging technologies to determine the representations of these MDD subtypes [12–15]. For example, studies focusing on intrinsic brain organization as assessed by resting-state functional magnetic resonance imaging (R-fMRI) revealed that compared to individuals with treatment-sensitive depression, individuals with treatment-resistant depression

¹The Center of Psychosomatic Medicine, Sichuan Provincial Center for Mental Health, Sichuan Provincial People's Hospital, University of Electronic Science and Technology of China, Chengdu, China. ²Institute of Brain and Psychological Sciences, Sichuan Normal University, Chengdu, China. ³School of Sport Training, Chengdu Sport University, Chengdu, China. ⁴School of Psychology, Shandong Normal University, Jinan, China. ⁵Department of Radiology and Huaxi MR Research Center (HMRR), Functional and Molecular Imaging Key Laboratory of Sichuan Province, West China Hospital of Sichuan University, Chengdu, China. ⁶Institute for Brain Research and Rehabilitation, South China Normal University, Guangzhou, China. ⁷The Clinical Hospital of Chengdu Brain Science Institute, MOE Key Laboratory for NeuroInformation, School of Life Science and Technology, University of Electronic Science and Technology of China, Chengdu, China. ⁸The Department of Psychology, The State Key Laboratory of Brain and Cognitive Sciences, The University of Hong Kong, Hong Kong, China. ⁹These authors contributed equally: Qi Liu, Xinqi Zhou. ¹⁰These authors jointly supervised this work: Benjamin Becker, Weihua Zhao.

✉email: ben_becker@gmx.de; zarazhao@uestc.edu.cn

Received: 1 January 2025 Revised: 6 May 2025 Accepted: 28 May 2025

Published online: 13 June 2025

showed hyperactivity in regions of the default mode network (DMN), hypoconnectivity within and between DMN regions, as well as aberrant activity and connectivity in the occipital lobe [16–18]. While resting-state fMRI has provided valuable insights into intrinsic functional alterations in MDD, task-based fMRI enables the examination of brain activity in response to specific cognitive or emotional demands, offering a complementary perspective on the neurobiological dysfunctions of MDD individuals. Impairments in social functioning, such as emotional perception and empathy, manifest as distinct behavioral patterns and neural representations across various MDD subtypes [19–21]. However, it is noteworthy that the observed subtypes which are typically determined through clinical assessments and genetic subgroups, might be driven by distinct neurophysiological underpinnings. Moreover, intervention studies using transcranial magnetic stimulation (TMS) targeting the dorsolateral prefrontal cortex (dlPFC), a key region of the frontoparietal network (FPN), have demonstrated heterogeneity in treatment efficacy, with therapeutic benefits observed only in around 50% MDD individuals. These findings underscore the necessity of a more precise, biologically informed framework for delineating MDD subtypes [22, 23]. The determination of neuroimaging-based subtypes of MDD has thus the potential to allow a more precise and biologically-informed definition of subtypes of intricate and clinically-relevant phenotypes. This, in turn, could facilitate the development of neuroimaging-based precise diagnostic methodologies and personalized therapeutic interventions.

The functional connectivity (FC) has been extensively employed to capture the intricate spatio-temporal structure of the functional organization of brain regions and networks. Its strength has been demonstrated to correlate with glucose metabolism and to undergo changes with age [24, 25]. Many neuroimaging studies have relied on static FC, derived from averaging R-fMRI or electroencephalography (EEG) time periods of 6–10 min, to investigate altered brain functional patterns among MDD subtypes [26–28]. However, static FC, defined as the degree of coherence between the blood-oxygen-level-dependent (BOLD) time-series of two brain regions across the entire scanning period, fails to adequately represent the complex temporal dynamics of brain function [26]. In contrast, model-based dynamic FC using dynamic conditional correlations (DCC) method can allowed us to estimate the instantaneous functional connectivity between all pairs of ROIs at each time point during the scan [24, 29, 30] with a higher retest reliability compared to traditional dynamic functional connectivity approach (i.e. sliding window). Furthermore, traditional case-control analyses, which primarily focus on group-level abnormalities, are insufficient for elucidating individual-level anomalies. The normative model, however, offers a pioneering statistical framework to characterize the biological developmental trajectory of neuroimaging features and to quantify individual deviations from this norm [26, 31, 32]. This approach provides valuable insights into inter-individual heterogeneity and aids the identification of neurobiological subtypes within psychiatric disorders. Consequently, in the current study, we employed both static and model-based dynamic FC as predictive variables for the first time in a normative model to comprehensively map the multilevel functional developmental trajectories of the human brain and characterize individual functional deviations in MDD.

Against this background, we employed a multi-faceted approach that integrated normative modeling and R-fMRI to quantify the neurobiological heterogeneity in MDD patients. Specifically, we parameterize this heterogeneity using multilevel (static and model-based dynamic) FC values as functional features. Our primary objective was to explore whether if subtype-specific neural representations in both R-fMRI and task-state fMRI exist (T-fMRI) (Fig. 1). We hypothesized that individuals with MDD would exhibit significant heterogeneity in FC deviation patterns across all levels, and that a more comprehensive understanding of these

deviations could be identified by examining multilevel FC features. Furthermore, we predicted that individuals with MDD could be clustered into different subgroups, characterized by unique patterns of multilevel FC deviations and task-based representations. Thus, we conducted a comprehensive investigation utilizing a large, multi-site R-fMRI dataset of 2428 participants (Dataset 1), as well as an independent cohort of 72 participants with both R-fMRI and T-fMRI data (Dataset 2). We first characterized the multilevel FC for each participant by computing static FC using Pearson correlation and model-based dynamic FC employing dynamic conditional correlation, which has been shown to possess a high level of test-retest reliability [24, 29, 33]. Next, we constructed normative models based on the multilevel FC features observed in HCs. These models were then employed to estimate individualized multilevel FC deviation maps for individuals with MDD. Following this, clustering analyses were applied to both the large, multi-site dataset and the independent cohort to identify potential MDD subtypes. Finally, we evaluated the imaging differences and task-based representation differences among the identified MDD subtypes. The comprehensive analytical pipeline overview of the current study is shown in Fig. 1.

METHODS

Participants

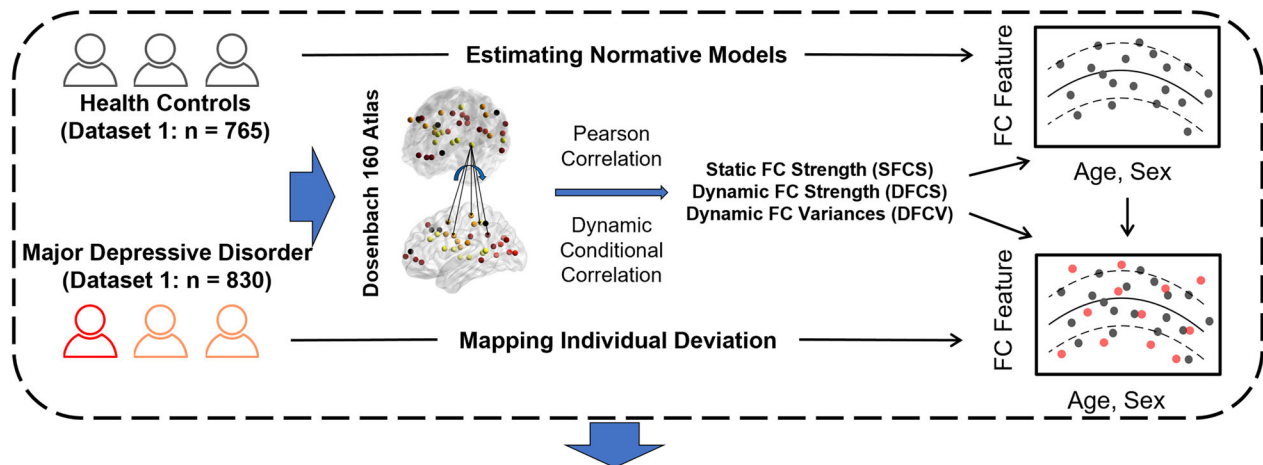
To investigate the resting-state multilevel functional heterogeneity and subtype-specific task-based representations of MDD, we included 2 independent cohorts: Dataset 1, referred to as the REST-meta-MDD cohort, included R-fMRI data from 1300 MDD patients and 1128 HCs collected by 25 Chinese research groups [34]. All participants in Dataset 1 provided information on diagnosis, age at scan, sex, education level, and for MDD patients, additional details such as first-episode or recurrent MDD, medication status, illness duration, and 17-item Hamilton Depression Rating Scale (HAM-D) scores. Dataset 2, an independent clinical cohort, contained R-fMRI and T-fMRI data from 37 first-episode, unmedicated MDD patients and 35 HCs [35–38]. This dataset included measures of diagnosis, age at scan, sex, education level, 21-item Beck Depression Inventory II (BDI-II) scores, and Interpersonal Reactivity Index-C (IRI-C) scores, which assess individual emotional empathy traits. To ensure data quality and consistency [34, 39], we excluded the participants from both datasets on predefined criteria: incomplete information, age outside the 18–65 range, poor spatial normalization quality, inadequate brain coverage, and excessive head motion. Additionally, we excluded sites with less than 10 individuals. After these exclusions, Dataset 1 comprised a sample of 830 MDD patients and 765 HCs from 16 research groups/sites, while Dataset 2 included 27 MDD patients and 31 HCs (more details see Table 1 and Table S1). The authors assert that all procedures contributing to this work comply with the ethical standards of the relevant national and institutional committees on human experimentation and with the Helsinki Declaration of 1975, as revised in 2013. All procedures involving participants were approved by the local ethical committees of participating centers (Dataset 1: respective local institutional review boards and ethics committees of REST-meta-MDD Consortium; Dataset 2: local ethics committee at the University of Electronic Science and Technology of China) and written informed consent was obtained from all participants.

Dataset 1: Characterization of MDD subtypes based on individual multilevel functional deviations

fMRI paradigms and data preprocessing. All participants in Dataset 1 underwent at least a T1-weighted structural scan and an R-fMRI scan, with the scan parameters detailed in Table 2. The structural MRI and R-fMRI data were preprocessed at each research group/site using a standardized DPARSF protocol (Supplement) [34].

Normative modeling of multilevel functional connectivity. To evaluate individual multilevel (i.e. static and model-based dynamic) functional connectivity, the average BOLD signals were extracted for the Dosenbach 160 regions of interest (ROIs) for each participant [40]. These ROIs were chosen based on their functional definition from five meta-analyses focusing on distinct cognitive domains, including error processing, default mode (task-induced deactivations), memory, language, and sensorimotor functions [40]. The Dosenbach's 160 atlas has demonstrated strong

A Estimation of the MDD individual deviation with normative models



B Identification of MDD subtypes and subtype differences

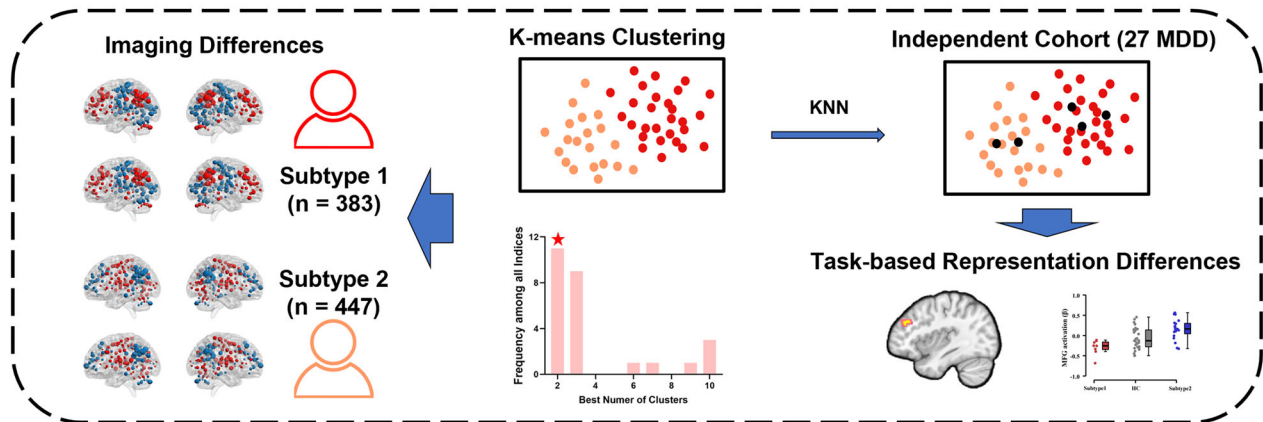


Fig. 1 Comprehensive analytical pipeline overview. **A** Estimation of major depressive disorder (MDD) individual deviation with normative models: Normative models are derived from the multilevel functional connectivity (FC) features of healthy controls (HCs) subjects. These models are then utilized to map MDD individuals, resulting in the MDD individual multilevel FC deviation map. **B** Identification of MDD subtypes and subtype differences: A K-means clustering algorithm is conducted to group MDD patients into distinct subtypes based on their individual multilevel FC deviation maps, and compare the imaging differences among the identified subtypes. The identified subtype labels are used to classify individual within the independent cohort into their respective subtypes by a K-Nearest Neighbors (KNN) algorithm and the task-based fMRI data was analyzed to explore representation differences among the identified subtypes.

sensitivity and reliability in detecting abnormal functional connectivity and network topology of MDD [34, 39]. The ROIs were further divided into six brain networks: the frontoparietal network (FPN), default mode network (DMN), cingulo-opercular network (CON), sensorimotor network (SMN), occipital network (ON), and cerebellar network (Cere). For each brain region, we used Pearson correlation to calculate static functional connectivity strength (SFCS) and dynamic conditional correlation [33] to estimate dynamic functional connectivity strength (DFCS) and dynamic functional connectivity variance (DFCV) (Supplement). Then, we developed normative models of these multilevel FC features (i.e. SFCS, DFCS and DFCV) as a function of age and sex, by using Gaussian process regression (GPR, Supplement) in the HCs [26, 31, 32]. To validate the generalizability of these models, we used a 10-fold cross-validation process prior to applying the trained models on MDD patients. Following this validation, the final normative models were trained on the entire healthy control cohort for subsequent analysis of functional deviation in MDD patients. To account for potential site effects and confounding factors, all functional connectivity features were modulated by a combat harmonization procedure that considered disease status, sex, age, years of education and mean framewise displacement as covariates.

Estimating individual multilevel functional deviations for MDD individuals. For each individual with MDD, we assessed their multilevel functional deviations by positioning their FC features onto the trained final normative

models from HCs. Specifically, we derived a Z-score for each FC feature to quantify the degree of deviation from the normative model. The Z-score was defined as follows:

$$Z = \frac{FC_{observed} - FC_{predicted}}{\sigma}$$

where $FC_{observed}$ represents the observed FC feature, $FC_{predicted}$ is the expected FC value estimated by the GPR, and σ is the square root of variance estimated from the GPR. Similarly, the individual multilevel functional deviation map of each HC was estimated by computing the Z-score during the 10-fold cross-validation. To identify significant individual-level FC deviations in participants, deviation maps were thresholded of $Z = \pm 2.58$ (corresponding to a p-value of <0.005), in line with previous studies [26, 41, 42].

Characterizing MDD subtypes based on individual multilevel functional deviations. A data-driven k-means clustering algorithm was used to determine MDD subtypes with multilevel FC features as clustering features. We varied the number of clusters (subtypes) from 2 to 10 and determined the optimal number of MDD subtypes using the NbClust package in R (Supplement) [43]. The leave-one-site-out validation was further conducted to evaluate the inter-site reproducibility of subtyping results. Subsequently, the brain deviations as well as demographic and clinical variables were further compared among the identified subtypes.

Table 1. Demographic and clinical characteristics of the participants.

Demographics	MDD	HC	p value
Dataset 1	830	765	
Age, years, mean (SD)	34.39 (11.58)	34.59 (13.13)	0.755 ^a
Sex, M/F	306/524	313/452	0.097 ^b
Education, years, mean (SD)	11.95 (3.36)	13.55 (3.43)	<0.001 ^a
First episode/ Recurrence	419/208		
Medicated/ unmedicated	222/314		
HAMD-17	21.28 (6.61) (n = 746)		
Dataset 2	27	31	
Age, years, mean (SD)	28.44 (8.22)	26.07 (8.41)	0.296 ^a
Sex, M/F	5/22	12/19	0.092 ^b
Education, years, mean (SD)	14.00 (3.28)	14.38 (2.90)	0.642 ^a
BDI-II	32.33 (9.42)		
IRI-total score	46.30 (10.11)		

MDD major depressive disorder, HC healthy control, SD standard deviation, M male, F female, BDI-II beck depression inventory II, IRI interpersonal reactivity index-C.

^ap value was calculated using two-sample t test.

^bp value was calculated using Chi-square test; all p values were corrected with FDR-correction.

Dataset 2: Specific task-based representations for identified MDD subtypes

MRI paradigms and data preprocessing. All participants in Dataset 2 underwent a T1-weighted structural scan, a 6.5 min R-fMRI scan, and two T-fMRI scans. The first T-fMRI scan lasted 7.3 min and involved a pain empathy task, where participants viewed physical pain stimuli (e.g. cutting a finger with a scissors) and affective pain stimuli (i.e. painful facial expressions), along with corresponding control stimuli (physical control, e.g. cutting papers with a scissors; affective control, neutral facial expression). During this task, participants were instructed to imagine the level of pain the person in the picture was experiencing. The second T-fMRI scan lasted 11.2 min and involved an implicit face processing task, where participants were asked to indicate the gender of faces displaying various emotional expressions, including angry, fearful, sad, neutral and happy. More details about the R-fMRI and the two T-fMRI scans are described in our previous studies [35, 37]. All MRI data in Dataset 2 were acquired via a 3.0 Tesla GE MR750 system (General Electric Medical System, Milwaukee, WI, USA) and were preprocessed with the standard DPARSF protocol similar with Dataset 1 (Supplement).

Identifying MDD subtypes with independent clinical cohort. To accurately identify individuals in Dataset 2 as the independent cohort into their respective MDD subtypes, we employed the K Nearest Neighbors (KNN) algorithm with a focus on FC features. The detailed steps taken were:

1. Feature Extraction: we calculated multilevel FC features (i.e. SFCS, DFCS and DFCV) for each MDD individual in Dataset 2 based on their R-MRI image.
2. Functional Deviation Estimation: we estimated the functional deviations for each MDD individual in Dataset 2 based on the normative models established from HC data in Dataset 1.
3. Classification Using KNN: we mapped the MDD individual in Dataset 2 to the subtyped MDD individuals of Dataset 1 by KNN (K = 1) algorithm with the functional deviations as classification features.

Validating subtype-specific task-based representations. To explore potential subtype-specific task-based neural representations during T-fMRI, we

conducted a General Linear Model (GLM) implemented in SPM 12 v7771 to analyze the pain empathy task and the implicit face processing task. On the individual level, two T-fMRI tasks were modeled with the canonical hemodynamic response function (HRF) on corresponding stimulus conditions (pain empathy: physical pain, affective pain, physical control and affective control; implicit face processing: angry, fearful, sad, neutral and happy). Additionally, contrast images of these T-fMRI tasks (pain empathy: [physical pain > physical control] and [affective pain > affective control]; implicit face processing: [angry > neutral], [fearful > neutral], [sad > neutral], [happy > neutral], [negative > neutral] and [positive > neutral]) were produced on the individual level for further intergroup comparison analyses. Small volume correction (SVC) with $p_{FWE} < 0.05$ correction at cluster level was conducted with bilateral dorsolateral prefrontal cortex (dlPFC) as ROI given the key role of dlPFC in emotion processing and as the target intervention region for MDD in previous studies [44, 45].

RESULTS

Individual deviations from normative models of multilevel functional connectivity in MDD

We conducted comprehensive analyses of FC for each participant, generating a total of 480 FC features through both static and model-based dynamic FC assessments. Normative models for these multilevel FC features were established derived from the Dataset 1 of 765 TD individuals (313 males, 18–64 years, Table 1), incorporating age and sex as arguments (see **Methods**). The robustness of these models was confirmed through 10-fold cross-validation, as indicated by standardized mean squared error (mean \pm SD: 1.002 ± 0.012) and mean squared log-loss (mean \pm SD: 0.002 ± 0.006) (Fig. S1). Correlation analyses between FC values and age revealed consistent age-related patterns across SFCS, DFCS, and DFCV levels, albeit with distinct patterns between genders (Fig. S2 and Fig. S3). After establishing robust normative models, we estimated the deviations of multilevel FC features from the established-normative models for each MDD individual ($n = 830$, 306 males, 18–65 years, Table 1). Relative to HCs, MDD individuals exhibited significant deviations in all three FC levels, with significantly larger positive deviations in the frontoparietal network (FPN), DMN and cingulo-opercular network (CON), and significantly larger negative deviations in the occipital network (ON), sensorimotor network (SMN) and CON (Fig. 2A, B). In addition, MDD individuals showed a greater number of extreme deviations (Fig. 2C), including greater extremely positive deviations in dynamic FC (i.e., DFCS and DFCV, Fig. 2D, E), and greater extremely negative deviations in static FC (i.e., SFCS, Fig. 2F, G). Notably, the combination of static and dynamic FC analyses identified a substantial majority (98.1%, $n = 814$) of MDD individuals showing extreme deviations from the established normative models in at least one multilevel FC feature. Specifically, 66.4% ($n = 551$) of MDD individuals showed extremely positive deviations, while 93.4% ($n = 775$) displayed extremely negative deviations (Fig. 2H). In contrast, when relying solely on static FC analysis, the identification rate for extreme deviations in MDD was notably lower (58.7% in total, $n = 487$). Further statistical analyses revealed that although there were considerable overlaps (6.3–33.7%, $n = 52$ –280) in the identification of extreme deviations across the three levels of FC features, there were also MDD individuals with FC-specific extreme deviations (Fig. 3A). These results revealed that both static and model-based dynamic FC contribute to mapping the functional abnormal patterns associated with MDD.

High heterogeneity in multilevel functional connectivity deviations among MDD individuals

To further examine the multilevel functional heterogeneity among individuals with MDD, we calculated the proportion exhibiting extreme deviations in each FC feature. Out of 480 FC features examined, a substantial portion FC features displayed extreme positive (74.6%, $n = 358$) or negative (82.7%, $n = 397$) deviations

Table 2. Scan parameters of the R-fMRI data from each site of Dataset 1.

Site	Scanner	Channel	TR (ms)	TE (ms)	FA (°)	FOV (mm ²)	Time Points	Voxel Size	Slices	Thickness (mm)	Gap (mm)
PKU	Siemens Trio 3 T	32	2000	30	90	210 × 210	210	3.28 × 3.28 × 4.80	30	4	0.8
SU	Philips Achieva 3 T	8	2000	30	90	240 × 240	200	1.67 × 1.67 × 4	37	4	0
ZJU	GE MR750	8	2000	30	90	220 × 220	184	2.29 × 2.29 × 3.20	37	3.2	0
CMU1	GE Signa 3 T	8	2000	30	90	240 × 240	200	3.75 × 3.75 × 3.00	35	3	0
JNU	GE MR750 3 T	8	2000	25	90	240 × 240	200	3.75 × 3.75 × 4.00	35	3	1
SMU	Siemens Trio 3 T	32	2000	30	90	240 × 240	212	3.75 × 3.75 × 4.52	32	3	1.52
CQMU1	GE Signa 3 T	8	2000	30	90	240 × 240	200	3.75 × 3.75 × 5.00	33	5	-
XJTU	GE Excite 1.5 T	16	2500	35	90	256 × 256	150	4.00 × 4.00 × 4.00	36	4	0
CSU	Siemens Trio 3 T	32	2500	25	90	240 × 240	200	3.75 × 3.75 × 3.50	39	3.5	0
SEU1	Siemens Verio 3.0 T	12	2000	25	90	240 × 240	240	3.75 × 3.75 × 4.00	36	4	0
CQMU2	GE Signa 3 T	8	2000	40	90	240 × 240	240	3.75 × 3.75 × 4.00	33	4	0
AMU	GE Signa 3 T	8	2000	22.5	30	220 × 220	240	3.44 × 3.44 × 4.60	33	4	0.6
SEU2	Siemens Trio 3 T	12	2000	30	90	220 × 220	242	3.44 × 3.44 × 4.00	32	3	1
CMU2	Siemens Trio 3 T	32	2000	30	90	200 × 200	240	3.12 × 3.12 × 4.20	33	3.5	0.7
CSU	Philips Achieva 3 T	32	2000	30	90	240 × 240	250	1.67 × 1.67 × 4	36	4	0
SCU	Philips Achieva 3 T TX	8	2000	30	90	240 × 240	240	3.75 × 3.75 × 4.00	36	4	0

TR repetition time, TE echo time, FA flip angle, FOV field of view, PKU peking university sixth hospital, SU the affiliated guangji hospital of soochow university, ZJU zhejiang university school of medicine, CMU1 china medical university, JNU the first affiliated hospital of jinan university, SMU first hospital of shanxi medical university, CQMU1 the first affiliated hospital of chongqing medical university (Qing-Hua Luo / Hua-Qing Meng group), XJTU the first affiliated hospital of xi'an jiaotong university, CSU the second xiangya hospital of central south university, SEU1 school of medicine: southeast university, CQMU2 the first affiliated hospital of chongqing medical university (Li Kuang group), AMU anhui medical university, SEU2 faculty of psychology: southwest university, CMU2 capital medical university, CSU second xiangya hospital of central south university, SCU west china hospital, sichuan university.

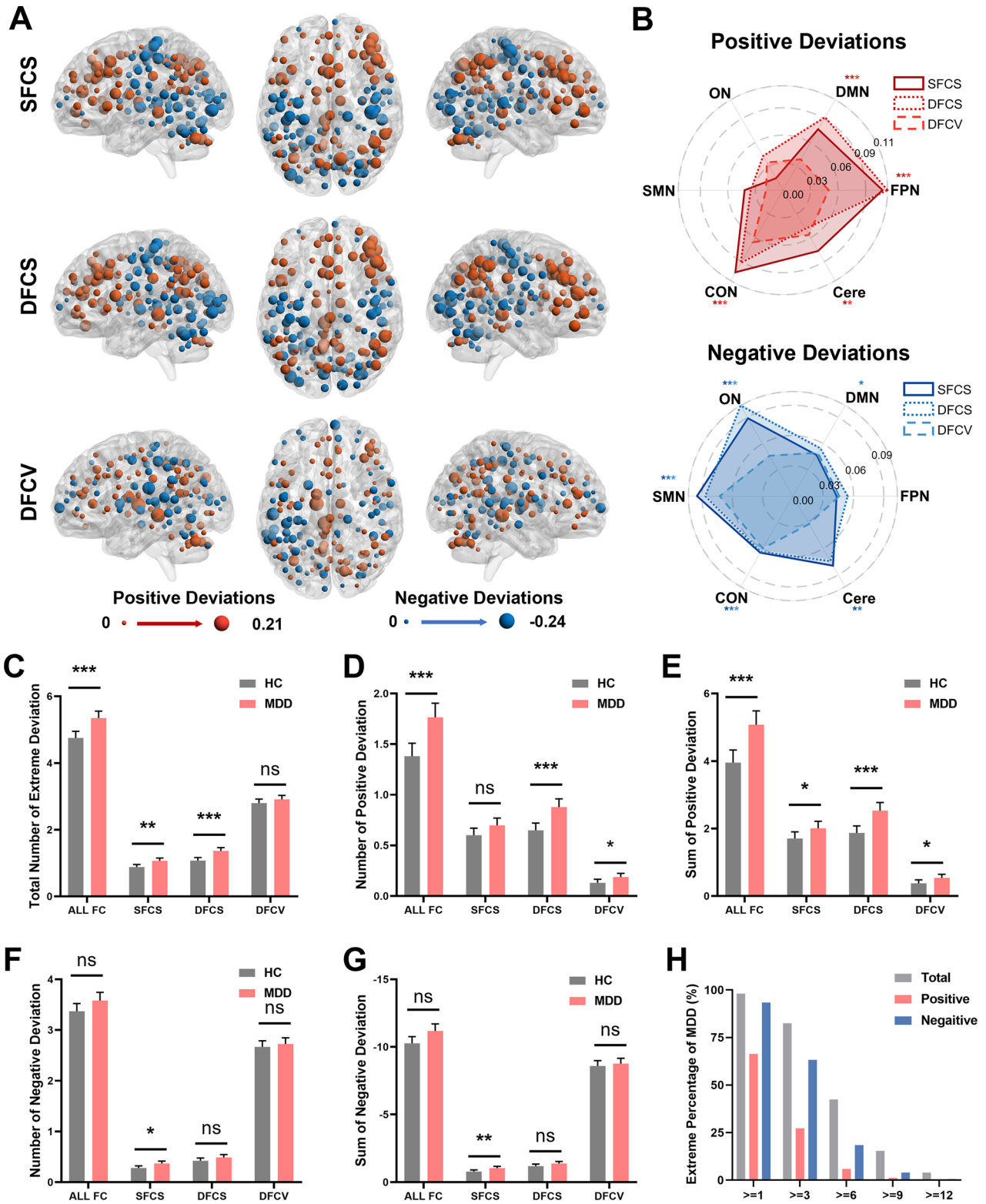


Fig. 2 Multilevel functional connectivity deviations from the established-normative models in major depressive disorder (MDD). **A, B** Region-level and network-level functional connectivity deviations in SFCS, DFCS and DFCV for MDD. * indicates that the network-level deviation of MDD significantly differs ($p_{FDR} < 0.5$) from healthy control in the functional connectivity corresponding to that color. **C–G** The total number differences of the overall deviation indices in multilevel functional connectivity between MDD and HCs. * $p < 0.05$, ** $p < 0.01$, *** $p < 0.001$, $^{ns}p > 0.05$, FDR corrected. **H** Bar plots show the distribution of the number of functional connectivity features per patient with extreme deviations. FC functional connectivity, SFCS static functional connectivity strength, DFCS dynamic functional connectivity strength, DFCV dynamic functional connectivity variance, FPN frontoparietal network, DMN default mode network, CON cingulo-opercular network, SMN sensorimotor network, ON occipital network, Cere cerebellar network. Error bars indicate 95% confidence interval.

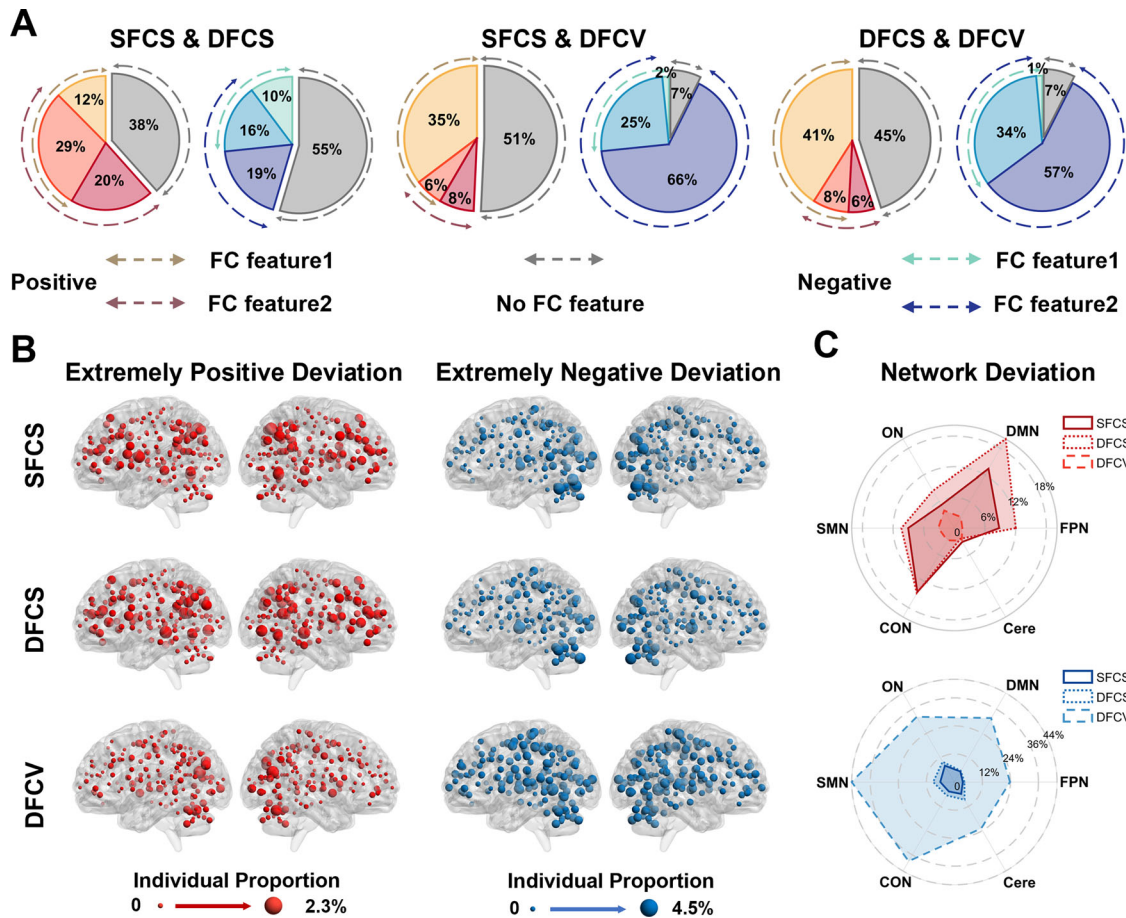


Fig. 3 The proportion of patients with major depressive disorder (MDD) with extreme deviation. **A** The proportion of MDD individuals with extreme deviation identified by each level of FC features and its overlaps across three levels of FC features. No FC feature represents that no FC feature at any level identified the presence of extreme deviation in these MDD individuals. **B** The proportion of MDD individuals with extreme deviation in single node at each FC feature-level, red spheres represent the extremely positive deviations and blue spheres represent the extremely negative deviations. **C** The proportion of MDD individuals with extreme deviation in network-level, top: extremely positive deviations, SFCS static functional connectivity strength, DFCS dynamic functional connectivity variance, FPN frontoparietal network, DMN default mode network, CON cingulo-opercular network, SMN sensorimotor network, ON occipital network, Cere cerebellar network.

in at least one MDD individual (Fig. 3B). However, when considering each FC feature individually, the percentage of MDD individuals exhibiting extreme deviations from the normative model was notably low, both for positive (2.3%, $n = 19$) and negative (4.5%, $n = 37$) deviations (Fig. 3B). At the network-level, extremely positive deviations in MDD were predominantly observed in the SFCS and DFCV features of FPN, DMN, SMN and CON ($n > 70$, 8.4%), while extremely negative deviations were more widespread across all six networks ($n > 190$, 22.9%), with particularly evident in the SMN and CON (Fig. 3C). These findings indicated that although alterations in FC are prevalent in the majority of MDD individuals, the specific FC features or brain regions exhibiting out-of-range alterations vary considerably among individual patients.

Multilevel functional connectivity deviation-based MDD subtypes

With multilevel FC deviations as clustering features, we classified the MDD individuals from Dataset 1 into two distinct subtypes (see **Methods**). This optimal subcluster number was consistently selected by 11 of 26 cluster criteria in the NbClust package (Fig. 4A). Furthermore, these subtyping results showed high reliability and reproducibility, as evidenced by the significantly greater similarity of functional deviations within the same subtype compared to those

between different subtypes ($p_{FDR} < 0.001$, Fig. 4B). Furthermore, there was no significant difference in the number of MDD subtypes across different sites ($\chi^2_{15} = 24.95$, $p = 0.051$, Fig. 4C, Table S2), and a high overlap rate (mean 97.1%, range: 93.8–98.9%, Fig. 4D) between the subtyping result of leave-one-site-out validation and the main subtyping result was observed.

In terms of functional deviation among the identified MDD subtypes, subtype 1 ($n = 383$, 46%) exhibited significantly more severe deviations compared to subtype 2 ($n = 447$, 54%) across all three levels FC features ($p_{FDR} < 0.001$, Fig. 4E and Table S3). Among individuals with MDD subtype 1, positive deviations were observed in the FPN and DMN, accompanied by negative deviations in the ON and SMN. Conversely, MDD subtype 2 individuals displayed a significantly opposite deviation pattern across all three levels of functional connectivity features ($p_{FDR} < 0.05$, Fig. 4F and Table S4–5). To evaluate the robustness of our clustering results, we conducted additional analyses by applying hierarchical clustering (Fig. S4), varying the number of clusters (Fig. S4), and performing clustering with both MDD and HC participants combined (Fig. S5). Consistently, the identified MDD subtypes demonstrated reproducible patterns of brain functional deviations across all methodological variations, reinforcing that the identified subtypes are independent of methodological choices. Further statistical comparisons revealed that MDD subtype 1 exhibited significantly higher extremely positive

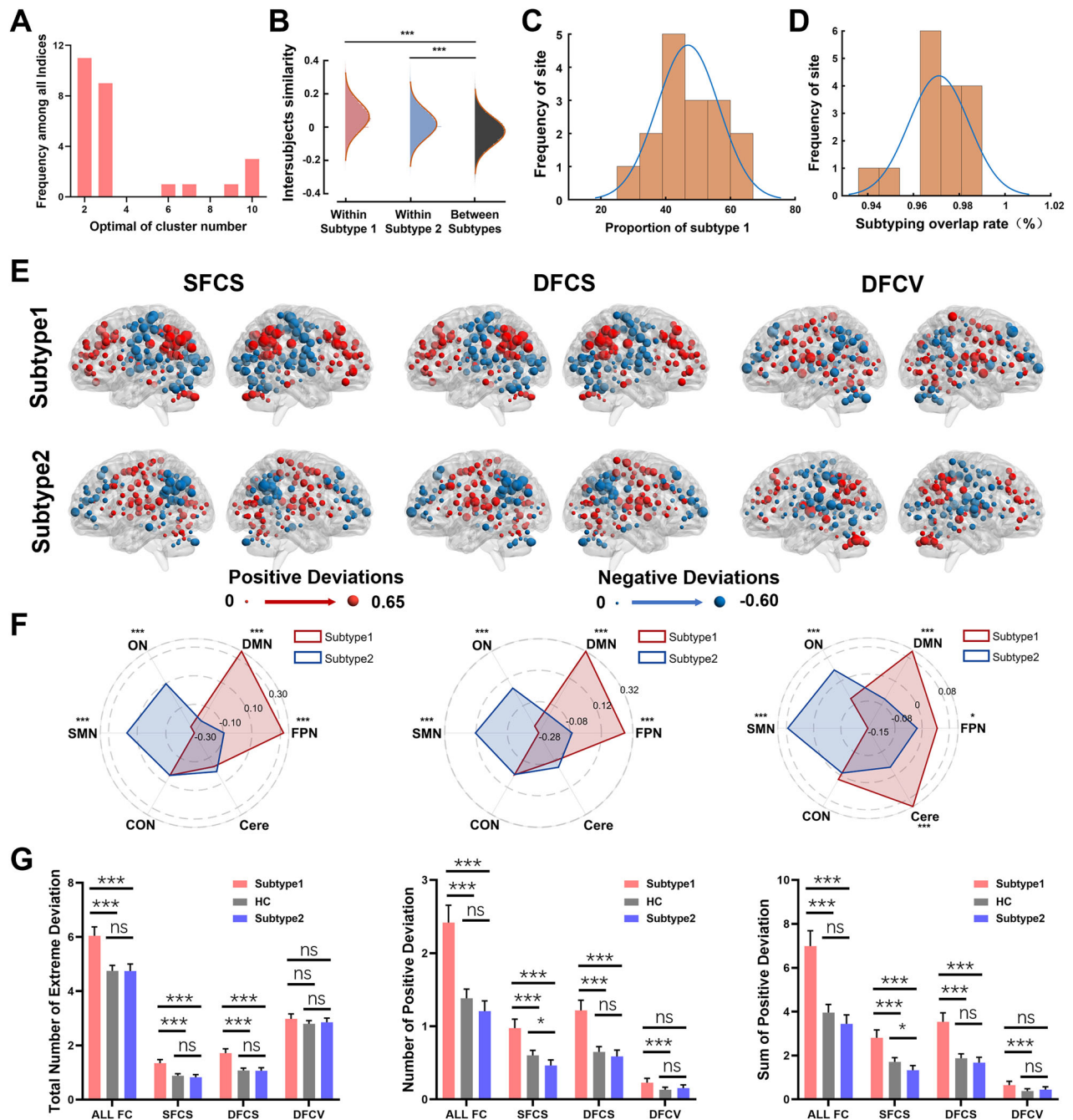


Fig. 4 Multilevel functional connectivity deviation-based MDD subtypes and their neuroimaging differences. **A** Determination of the optimal subtype number of MDD using the NbClust package. **B** The inter-subject similarity of functional deviations within MDD single subtype and between MDD subtypes. **C** Distribution of the proportion of MDD subtype 1 in subtyping results. **D** Distribution of the overlap rates between the subtyping result of leave-one-site-out validation and the main subtyping result. **E, F** Region-level and network-level functional connectivity deviations in SFCS, DFCS and DFCV for each MDD subtype. * indicates that there was a significant difference on the network-level deviation between MDD subtypes. **G** The between-group differences of the overall deviation indices in multilevel functional connectivity among MDD subtypes and HCs. * $p < 0.05$, *** $p < 0.001$, ^{ns} $p > 0.05$, FDR corrected. SFCS static functional connectivity strength, DFCS dynamic functional connectivity strength, DFCV dynamic functional connectivity variance, FPN frontoparietal network, DMN default mode network, CON cingulo-opercular network, SMN sensorimotor network, ON occipital network, Cere cerebellar network. Error bars indicate 95% confidence interval.

deviations compared to those with MDD subtype 2 for SFCS and DFCS features ($p_{FDR} < 0.001$, Fig. 4G), particularly in the FPN, DMN and CON (Fig. S6). Nevertheless, no significant differences were observed between the two subtypes in terms of the burden of depression ($t_{(744)} = 0.415$, $p = 0.678$), medicated proportion ($\chi^2 = 0.161$, $p = 0.688$) or first-episode proportion ($\chi^2 = 0.458$, $p = 0.499$). These findings suggested that MDD patients, despite sharing the same

diagnosis, may exhibit varying abnormal patterns of functional deviations.

Subtype-specific representations in depression-related tasks

We further investigated whether there were any subtype-specific neural representations in depression-related tasks. The MDD individuals in the independent cohort ($n = 27$, 5 males, Table 1) were also

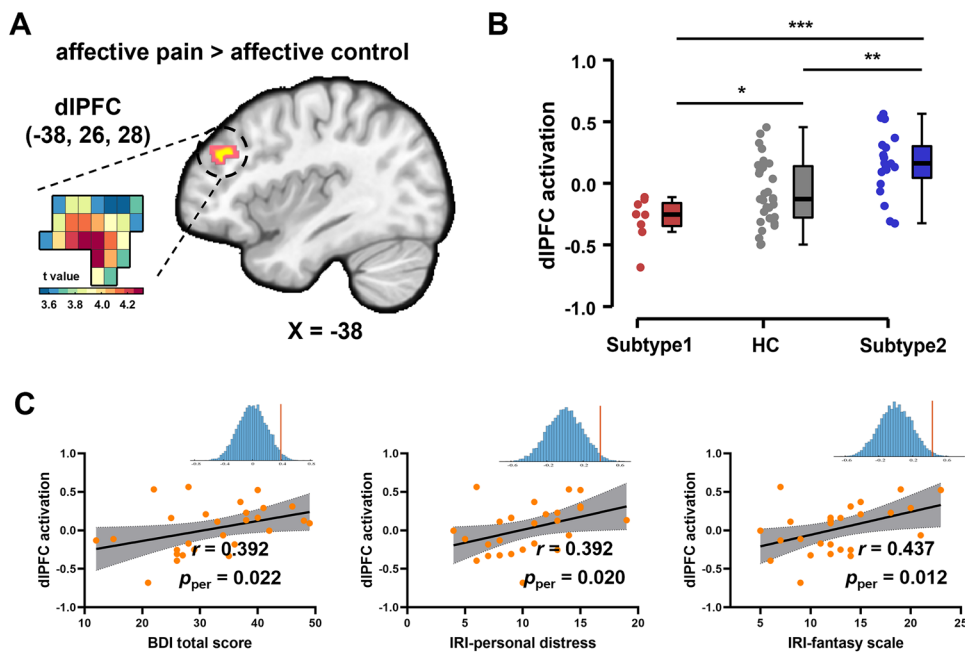


Fig. 5 Subtype-specific representation in pain empathy task. **A** The differences between two MDD subtypes (subtype 2 > subtype 1) in neural response of dorsolateral prefrontal cortex (dlPFC) to affective pain > affective control. **B** The post-hoc t-tests among two MDD subtypes and HCs on the activation of dlPFC to affective pain > affective control. * $p < 0.05$, ** $p < 0.01$, *** $p < 0.001$, FDR corrected. **C** Correlation analyses revealed significant correlations the activation of dlPFC to affective pain > affective control and the BDI total score, IRI-personal distress, and IRI-fantasy scale. The blue histogram represents the distribution of correlation coefficients obtained from 10,000 permutation tests, and the red line represents the original correlation coefficient. HC healthy control, BDI Beck Depression Inventory II, IRI Interpersonal Reactivity Index-C.

categorized into two subtypes (subtype 1 = 8, subtype 2 = 19) using the KNN algorithm based on the subtyping results from Dataset 1 (see **Methods**). This subtyping result also demonstrated high reliability, as indicated by the substantial overlap rate (mean 97.8%, range: 92.6–100%, Table S6) between the subtyping result obtained with different K values of the KNN algorithm and the primary subtyping outcome. In addition, the two subtypes in the independent cohort did not differ in age, sex, education, IRI total score and its subscales ($p_s > 0.211$, Table S7), while there was a significant difference in BDI score (mean \pm SD: subtype 1 = 24.000 ± 7.597 ; subtype 2 = 35.842 ± 7.869 , $p_{FDR} = 0.013$). For the pain empathy task, whole-brain intergroup comparison analyses revealed higher activation in the dorsolateral prefrontal cortex (dlPFC, MNI peak coordinate: $-38, 26, 28$, $k = 90$, $p_{FWE-SVC} = 0.029$, Fig. 5A) for MDD subtype 2 than subtype 1 during the affective pain > affective control condition. There were no significant differences between two MDD subtypes for other conditions in the pain empathy task or implicit face processing task. Post-hoc t-tests, comparing this dlPFC activation between MDD individuals and HCs, revealed that the activation for HCs was significantly higher than MDD subtype 1 ($t_{(37)} = 2.169$, $p_{FDR} = 0.037$), but significantly lower than MDD subtype 2 ($t_{(48)} = -3.041$, $p_{FDR} = 0.006$). However, there was no significant difference between the entire MDD group and HCs ($t_{(56)} = 1.306$, $p_{FDR} = 0.197$) (Fig. 5B). Finally, exploratory correlation analyses found that the activation of dlPFC during the affective pain > affective control condition in individuals with MDD was positively correlated with the burden of depression ($r = 0.392$, $p_{per} = 0.022$), IRI-personal distress scores ($r = 0.392$, $p_{per} = 0.020$), and IRI-fantasy scores ($r = 0.437$, $p_{per} = 0.012$) (Fig. 5C), with 10000 permutation tests. These findings suggest subtype-specific neural patterns in depression-related social tasks and potential links with depression severity and empathy-related traits.

DISCUSSION

This study combined normative modelling of a large multi-site R-fMRI dataset of 765 HCs and 830 MDD patients with original data

from a sample of non-medicated well-characterized MDD patients to characterize the developmental trajectory of brain multilevel functional features and quantitatively map the individual deviations in multilevel FC features in MDD. Notably, two reproducible MDD subtypes were identified and validated in an independent cohort of 27 MDD patients, demonstrating opposing neural representations in both R-fMRI and T-fMRI. Our findings emphasize the synergistic contribution of static and model-based dynamic FC in delineating the aberrant functional deviations in MDD individuals. Crucially, although the two identified MDD subtypes did not differ in clinical symptom severity, they displayed diametrically opposed patterns of multilevel brain functional deviations and neural representations of emotional empathy. This observation substantially advances our understanding of the neurobiological heterogeneity of MDD, and offers promising implications for the development of precise neuroimaging-based diagnostic methodologies and personalized therapeutic interventions.

The normative model provided a robust statistical framework for quantitatively assessing individual deviations from the typical neurobiological developmental patterns throughout life. With this model, we were able to estimate individual functional deviations and to identify extreme deviation features for each patient with MDD, respectively. At the group level, we observed statistically significant positive deviations across all three levels of FC features in the FPN and DMN regions in MDD compared to HCs. These hyperconnectivities in the FPN and DMN have been associated with impaired cognitive functioning, difficulty concentrating, and increased self-referential processing in MDD patients [26, 46, 47]. Conversely, significant negative deviations were observed in ON and SMN regions in MDD, which may correspond to reduced visual information processing and motor coordination difficulties [46, 47]. Notably, MDD exhibited compound abnormalities in the CON and cerebellum, characterized by both positive and negative deviations compared to HCs. This bidirectional abnormality may reflect the dual challenges of emotional and motor functioning in MDD and the complex neural adaptations the brain undertakes in

response to these challenges [48, 49]. At the individual level, a higher proportion of MDD patients exhibiting dynamic hyperconnectivity compared to HCs were identified. This excessive temporal variability in brain function has been associated with increased frequencies of spontaneous, internally orientated cognition processes in MDD [50–52]. Even more significantly, the combination of model-based dynamic and static FC features identified abnormal functional deviations in over 98% of MDD patients, significantly outperforming static FC analysis alone, which had an identification rate of only 58.7%. These findings highlight complementary nature of these two approaches in understanding brain function. However, the overlap between these abnormal features was remarkably low, revealing the high degree of neurobiological heterogeneity among MDD patients.

Using a functional deviation-based data-driven approach, we identified two MDD subtypes characterized by homogeneous deviation orientations at multilevel FC features: the FPN-DMN dominant subtype and the ON-SMN dominant subtype. The FPN-DMN dominant subtype exhibited a pattern of positive functional deviations in the DMN and FPN, coupled with negative deviations in the ON and the SMN. Conversely, the ON-SMN dominant subtype showed an inverse pattern of deviations in these respective regions. The observed divergence in brain function between these two subtypes may elucidate the limited success of neurostimulation treatments to fully ameliorate symptoms to healthy levels in up to two-thirds of MDD patients [53, 54]. In particular, the opposing functional representations of the DMN and FPN in the two subtypes may potentially explain why only around 50% of MDD patients respond favorably to transcranial magnetic stimulation (TMS) interventions, as TMS primarily aims to decrease the functional activity of these two networks [22, 23, 55, 56]. This suggests that TMS may only be effective for a subset of MDD patients, underscoring the need for subtype-specific treatment approaches [28]. Consistent with previous studies, we did not find differences in clinical symptoms between the two identified subtypes, despite their notable variations in the severity of brain functional deviations [26, 28]. This finding indicates the possibility that homogeneous symptom representations can coexist alongside heterogeneous representations of brain function. Future studies should incorporate more refined behavioral and clinical assessments to better differentiate these subtypes and identify potential distinctions that may be overlooked by conventional measures. Moreover, although the ON-SMN dominant subtype exhibited significant functional deviations, the degree of these deviations was less extreme compared to HCs. This observation is consistent with the contracted connectome hierarchy observed in patients with MDD [57].

Subsequently, we were able to robustly classify individual subtypes in the independent cohort as well. Unlike our above findings that only indicated a trend in depression burden between our defined two subtypes, this difference became statistically significant in the independent cohort. Possible reasons for this include the smaller sample size of the independent cohort ($N = 27$) and the use of a self-report depression assessment scale (i.e., BDI-II) in the independent cohort, which may have overestimated the difference between the two subtypes compared to a professional, structured assessment instrument (i.e., HAM-D) [58–61]. Besides differences in functional representation on R-fMRI, the two subtypes exhibited inverse representations compared to HCs in the dorsolateral prefrontal cortex, during emotional pain empathy. Notably, there was no significant difference between the entire MDD group and HCs, highlighting the significance of subtyping using the current models. Moreover, exploratory analyses have shown that the activation of this region is associated with depressive burden and empathic traits in individuals with MDD. These findings echo the role of the dIPFC in emotional reappraisal, impulse control, and emotion regulation that are commonly impaired in MDD [62, 63]. Importantly, TMS

interventions targeting the dIPFC have been shown to enhance pain empathy and reduce anhedonia in a subset of patients with MDD [45, 64]. Thus, the future TMS interventions targeting the dIPFC should take into account the neuroimaging-based subtype to tailor the treatment strategy accordingly (increase vs. decrease). Additionally, we did not find any differences in behavior or neural activation between the two subtypes during the implicit face processing task, which may be attributed to the implicit nature of the present paradigm.

Limitations

Several limitations of the study should be acknowledged. Firstly, we mapped the multilevel brain functional developmental trajectories for individuals aged 18–65 due to the limited availability of data for individuals outside this age range. Future studies should incorporate data from a broader and more evenly distributed age range to map functional developmental trajectories across the entire lifespan. Secondly, the current study identified two MDD subtypes with distinct resting-state and task-based functional representations using exclusively Chinese samples. However, due to the cultural homogeneity of the sample and the limited amount of task-based fMRI data, future studies should aim to replicate and extend these findings in larger task-based datasets and more diverse populations. Thirdly, the effects of neurostimulation and pharmacological treatments on these neurobiological subtypes should be further evaluated to guide personalized interventions. Finally, integrating more comprehensive individual information, including brain imaging, genetic, environmental, and cognitive-behavioral data, could provide a more thorough understanding of MDD heterogeneity.

CONCLUSIONS

In summary, we employed a multilevel rather than single level data-driven approach to identify neurobiological subtypes of MDD that exhibited distinct resting-state and task-based functional representations. This approach aimed to elucidate the critical heterogeneity in MDD, despite similar symptoms among subtypes. Our study highlights the importance of the multilevel FC analysis framework for understanding the complex heterogeneity of brain function in patients with MDD. Not only does this approach provide valuable insights into the neurobiological underpinnings of the disorder, but it also has implications for the development of more personalized diagnostic and therapeutic approaches tailored to the specific neurobiological subtype of each patient. Future studies should further validate and generalize these findings to diverse populations and evaluate the impact of different treatments on these neurobiological subtypes.

DATA AVAILABILITY

For the discovery cohort (Dataset 1), all data required for reproducing our findings have been publicly available. Details and access information are provided at <http://rfmri.org/REST-meta-MDD>. The resting-state and task-state fMRI data of validation cohort (Dataset 2) that support the findings of this study are available on request from the corresponding authors.

CODE AVAILABILITY

Software packages used in this manuscript include DPARSF (<http://rfmri.org/DPARSF>), Dynamic Conditional Correlation (https://github.com/canlab/Lindquist_Dynamic_Correlation), ComBat harmonization (https://github.com/Jfortin1/ComBat_Harmonization), Normative modelling (https://pcntoolkit.readthedocs.io/en/latest/pages/normative_modelling_walkthrough.html) and NbClust (<https://www.rdocumentation.org/packages/NbClust/versions/3.0.1/topics/NbClust>). The codes used in this study are available on request from the corresponding authors.

REFERENCES

- Ferrari AJ, Santomauro DF, Mantilla Herrera AM, Shadid J, Ashbaugh C, Erskine HE, et al. Global, regional, and national burden of 12 mental disorders in 204 countries and territories, 1990–2019: a systematic analysis for the Global Burden of Disease Study 2019. *Lancet Psychiatry*. 2022;9:137–50. [https://doi.org/10.1016/S2215-0366\(21\)00395-3](https://doi.org/10.1016/S2215-0366(21)00395-3).
- Kupfer DJ, Frank E, Phillips ML. Major depressive disorder: new clinical, neurobiological, and treatment perspectives. *Lancet*. 2012;379:1045–55. [https://doi.org/10.1016/S0140-6736\(11\)60602-8](https://doi.org/10.1016/S0140-6736(11)60602-8).
- Lu J, Xu X, Huang Y, Li T, Ma C, Xu G, et al. Prevalence of depressive disorders and treatment in China: a cross-sectional epidemiological study. *Lancet Psychiatry*. 2021;8:981–90. [https://doi.org/10.1016/S2215-0366\(21\)00251-0](https://doi.org/10.1016/S2215-0366(21)00251-0).
- Malhi GS, Mann JJ. Depression. *Lancet*. 2018;392:2299–312. [https://doi.org/10.1016/S0140-6736\(18\)31948-2](https://doi.org/10.1016/S0140-6736(18)31948-2).
- Moussavi S, Chatterji S, Verdes E, Tandon A, Patel V, Ustun B. Depression, chronic diseases, and decrements in health: results from the World Health Surveys. *Lancet*. 2007;370:851–8. [https://doi.org/10.1016/S0140-6736\(07\)61415-9](https://doi.org/10.1016/S0140-6736(07)61415-9).
- Nordentoft M, Mortensen PB, Pedersen CB. Absolute risk of suicide after first hospital contact in mental disorder. *Arch Gen Psychiatry*. 2011;68:1058–64. <https://doi.org/10.1001/archgenpsychiatry.2011.113>.
- Tone EB, Tully EC. Empathy as a “risky strength”: a multilevel examination of empathy and risk for internalizing disorders. *Dev Psychopathol*. 2014;26:1547–65. <https://doi.org/10.1017/S0954579414001199>.
- American Psychiatric Association. Diagnostic and statistical manual of mental disorders. 5th Edn. American Psychiatric Association; Washington, DC, 2013. <https://doi.org/10.1176/appi.books.9780890425596>.
- Harald B, Gordon P. Meta-review of depressive subtyping models. *J Affect Disord*. 2012;139:126–40. <https://doi.org/10.1016/j.jad.2011.07.015>.
- Penninx BWJH, Lamers F, Milaneschi Y. Clinical heterogeneity in major depressive disorder. *Eur Neuropsychopharmacol*. 2018;28:559–560. <https://doi.org/10.1016/j.euroneuro.2017.12.090>.
- Rush AJ. The varied clinical presentations of major depressive disorder. *J Clin Psychiatry*. 2007;68:22132.
- Diego-Adeliño, de J, Pires P, Gómez-Ansón B, Serra-Blasco M, Vives-Gilbert Y, et al. Microstructural white-matter abnormalities associated with treatment resistance, severity and duration of illness in major depression. *Psychol Med*. 2014;44:1171–82. <https://doi.org/10.1017/S003329171300158X>.
- Li M, Wu F, Cao Y, Jiang X, Kong L, Tang Y. Abnormal white matter integrity in Papez circuit in first-episode medication-naïve adults with anxious depression: a combined voxel-based analysis and region of interest study. *J Affect Disord*. 2023;324:489–95. <https://doi.org/10.1016/j.jad.2022.12.149>.
- Olvet DM, Peruzzo D, Thapa-Chhetry B, Sublette ME, Sullivan GM, Oquendo MA, et al. A diffusion tensor imaging study of suicide attempters. *J Psychiatr Res*. 2014;51:60–67. <https://doi.org/10.1016/j.jpsychires.2014.01.002>.
- Zhao P, Wang X, Wang Q, Yan R, Chattun MR, Yao Z, et al. Altered fractional amplitude of low-frequency fluctuations in the superior temporal gyrus: a resting-state fMRI study in anxious depression. *BMC Psychiatry*. 2023;23:847. <https://doi.org/10.1186/s12888-023-05364-w>.
- Guo W, Liu F, Xue Z, Gao K, Liu Z, Xiao C, et al. Decreased interhemispheric coordination in treatment-resistant depression: a resting-state fMRI study. *PLoS ONE*. 2013;8:e71368. <https://doi.org/10.1371/journal.pone.0071368>.
- He Z, Cui Q, Zheng J, Duan X, Pang Y, Gao Q, et al. Frequency-specific alterations in functional connectivity in treatment-resistant and -sensitive major depressive disorder. *J Psychiatr Res*. 2016;82:30–39. <https://doi.org/10.1016/j.jpsychires.2016.07.011>.
- Runia N, Yücel DE, Lok A, de Jong K, Denys DAJP, van Wingen GA, et al. The neurobiology of treatment-resistant depression: a systematic review of neuroimaging studies. *Neurosci Biobehav Rev*. 2022;132:433–48. <https://doi.org/10.1016/j.neubiorev.2021.12.008>.
- Guo CC, Hyett MP, Nguyen VT, Parker GB, Breakspear MJ. Distinct neurobiological signatures of brain connectivity in depression subtypes during natural viewing of emotionally salient films. *Psychol Med*. 2016;46:1535–45. <https://doi.org/10.1017/S0033291716000179>.
- Guhn A, Merkel L, Hübner L, Dziobek I, Sterzer P, Köhler S. Understanding versus feeling the emotions of others: how persistent and recurrent depression affect empathy. *J Psychiatr Res*. 2020;130:120–7. <https://doi.org/10.1016/j.jpsychires.2020.06.023>.
- Kustubayeva A, Eliassen J, Matthews G, Nelson E. fMRI study of implicit emotional face processing in patients with MDD with melancholic subtype. *Front Hum Neurosci*. 2023;17:1029789. <https://doi.org/10.3389/fnhum.2023.1029789>.
- Berlim MT, Van Den Eynde F, Tovar-Perdomo S, Daskalakis ZJ. Response, remission and drop-out rates following high-frequency repetitive transcranial magnetic stimulation (rTMS) for treating major depression: a systematic review and meta-analysis of randomized, double-blind and sham-controlled trials. *Psychol Med*. 2014;44:225–39. <https://doi.org/10.1017/S0033291713000512>.
- Taylor SF, Gu P, Simmonite M, Lasagna C, Tso IF, Lee TG, et al. Lateral prefrontal stimulation of active cortex with theta burst transcranial magnetic stimulation affects subsequent engagement of the frontoparietal network. *Biol Psychiatry Cogn Neurosci Neuroimaging*. 2024;9:235–44. <https://doi.org/10.1016/j.bpsc.2023.10.005>.
- Choe AS, Nebel MB, Barber AD, Cohen JR, Xu Y, Pekar JJ, et al. Comparing test-retest reliability of dynamic functional connectivity methods. *Neuroimage*. 2017;158:155–75. <https://doi.org/10.1016/j.neuroimage.2017.07.005>.
- Castrillon G, Epp S, Bose A, Fraticelli L, Hechler A, Belenya R, et al. An energy costly architecture of neuromodulators for human brain evolution and cognition. *Sci Adv*. 2023;9:eadi7632. <https://doi.org/10.1126/sciadv.adi7632>.
- Sun X, Sun J, Lu X, Dong Q, Zhang L, Wang W, et al. Mapping neurophysiological subtypes of major depressive disorder using normative models of the functional connectome. *Biol Psychiatry*. 2023;94:936–47. <https://doi.org/10.1016/j.biopsych.2023.05.021>.
- Wang Q, He C, Wang Z, Fan D, Zhang Z, Xie C, et al. Connectomics-based resting-state functional network alterations predict suicidality in major depressive disorder. *Transl Psychiatry*. 2023;13:365. <https://doi.org/10.1038/s41398-023-02655-4>.
- Zhang Y, Wu W, Toll RT, Naparstek S, Maron-Katz A, Watts M, et al. Identification of psychiatric-disorder subtypes from functional-connectivity patterns in resting-state electroencephalography. *Nat Biomed Eng*. 2020. <https://doi.org/10.1038/s41551-020-00614-8>.
- Engle R. Dynamic conditional correlation: a simple class of multivariate generalized autoregressive conditional heteroskedasticity models. *J Bus Econ Stat*. 2002;20:339–50. <https://doi.org/10.1198/073500102288618487>.
- Lindquist MA, Xu Y, Nebel MB, Caffo BS. Evaluating dynamic bivariate correlations in resting-state fMRI: a comparison study and a new approach. *Neuroimage*. 2014;101:531–46. <https://doi.org/10.1016/j.neuroimage.2014.06.052>.
- Marquand AF, Rezek I, Buitelaar J, Beckmann CF. Understanding heterogeneity in clinical cohorts using normative models: beyond case-control studies. *Biol Psychiatry*. 2016;80:552–61. <https://doi.org/10.1016/j.biopsych.2015.12.023>.
- Shan X, Uddin LQ, Xiao J, He C, Ling Z, Li L, et al. Mapping the heterogeneous brain structural phenotype of autism spectrum disorder using the normative model. *Biol Psychiatry*. 2022;91:967–76. <https://doi.org/10.1016/j.biopsych.2022.01.011>.
- Kim J, Andrews-Hanna JR, Eisenbarth H, Lux BK, Kim HJ, Lee E, et al. A dorsomedial prefrontal cortex-based dynamic functional connectivity model of rumination. *Nat Commun*. 2023;14:3540. <https://doi.org/10.1038/s41467-023-39142-9>.
- Yan C-G, Chen X, Li L, Castellanos FX, Bai T-J, Bo Q-J, et al. Reduced default mode network functional connectivity in patients with recurrent major depressive disorder. *Proc Natl Acad Sci*. 2019;116:9078–83. <https://doi.org/10.1073/pnas.1900390116>.
- Chen Y, Liu C, Xin F, Zou H, Huang Y, Wang J, et al. Opposing and emotion-specific associations between frontal activation with depression and anxiety symptoms during facial emotion processing in generalized anxiety and depression. *Prog Neuropsychopharmacol Biol Psychiatry*. 2023;123:110716. <https://doi.org/10.1016/j.pnpbp.2023.110716>.
- Liu Q, Zhou B, Zhang X, Qing P, Zhou X, Zhou F, et al. Abnormal multi-layered dynamic cortico-subcortical functional connectivity in major depressive disorder and generalized anxiety disorder. *J Psychiatr Res*. 2023;167:23–31. <https://doi.org/10.1016/j.jpsychires.2023.10.004>.
- Xu X, Dai J, Liu C, Chen Y, Xin F, Zhou F, et al. Common and disorder-specific neurofunctional markers of dysregulated empathic reactivity in major depression and generalized anxiety disorder. *Psychother Psychosom*. 2020;89:114–6. <https://doi.org/10.1159/000504180>.
- Xu X, Xin F, Liu C, Chen Y, Yao S, Zhou X, et al. Disorder- and cognitive demand-specific neurofunctional alterations during social emotional working memory in generalized anxiety disorder and major depressive disorder. *J Affect Disord*. 2022;308:98–105. <https://doi.org/10.1016/j.jad.2022.04.023>.
- Yang H, Chen X, Chen Z-B, Li L, Li X-Y, Castellanos FX, et al. Disrupted intrinsic functional brain topology in patients with major depressive disorder. *Mol Psychiatry*. 2021;26:7363–71. <https://doi.org/10.1038/s41380-021-01247-2>.
- Dosenbach NUF, Nardos B, Cohen AL, Fair DA, Power JD, Church JA, et al. Prediction of Individual Brain Maturity Using fMRI. *Science*. 2010;329:1358–61. <https://doi.org/10.1126/science.1194144>.
- Wolfers T, Doan NT, Kaufmann T, Alnæs D, Moberget T, Agartz I, et al. Mapping the heterogeneous phenotype of schizophrenia and bipolar disorder using normative models. *JAMA Psychiatry*. 2018;75:1146–55. <https://doi.org/10.1001/jamapsychiatry.2018.2467>.
- Wolfers T, Beckmann CF, Hoogman M, Buitelaar JK, Franke B, Marquand AF. Individual differences v. the average patient: mapping the heterogeneity in ADHD using normative models. *Psychol Med*. 2020;50:314–23. <https://doi.org/10.1017/S0033291719000084>.
- Charrad M, Ghazzali N, Boiteau V, Niknafs A. NbClust: an R package for determining the number of clusters in a data set. *J Stat Softw*. 2014;61:1–36. <https://doi.org/10.18637/jss.v061.i06>.

44. Molavi P, Azizaram S, Basharpour S, Atadokht A, Nitsche MA, Salehinejad MA. Repeated transcranial direct current stimulation of dorsolateral-prefrontal cortex improves executive functions, cognitive reappraisal emotion regulation, and control over emotional processing in borderline personality disorder: A randomized, sham-controlled, parallel-group study. *J Affect Disord.* 2020;274:93–102. <https://doi.org/10.1016/j.jad.2020.05.007>.
45. Light SN, Bieliauskas LA, Taylor SF. Measuring change in anhedonia using the “Happy Faces” task pre- to post-repetitive transcranial magnetic stimulation (rTMS) treatment to left dorsolateral prefrontal cortex in Major Depressive Disorder (MDD): relation to empathic happiness. *Transl Psychiatry.* 2019;9:1–10. <https://doi.org/10.1038/s41398-019-0549-8>.
46. Zhang J, Wang J, Wu Q, Kuang W, Huang X, He Y, et al. Disrupted brain connectivity networks in drug-naive, first-episode major depressive disorder. *Biol Psychiatry.* 2011;70:334–42. <https://doi.org/10.1016/j.biopsych.2011.05.018>.
47. Yang Y, Zhu D, Zhang C, Zhang Y, Wang C, Zhang B, et al. Brain structural and functional alterations specific to low sleep efficiency in major depressive disorder. *Front Neurosci.* 2020;14:50. <https://doi.org/10.3389/fnins.2020.00050>.
48. Dai P, Zhou X, Xiong T, Ou Y, Chen Z, Zou B, et al. Altered effective connectivity among the cerebellum and cerebrum in patients with major depressive disorder using multisite resting-state fMRI. *Cerebellum.* 2023;22:781–9. <https://doi.org/10.1007/s12311-022-01454-9>.
49. Wang X, Xia J, Wang W, Lu J, Liu Q, Fan J, et al. Disrupted functional connectivity of the cerebellum with default mode and frontoparietal networks in young adults with major depressive disorder. *Psychiatry Res.* 2023;324:115192. <https://doi.org/10.1016/j.psychres.2023.115192>.
50. Sun J, Liu Z, Rolls ET, Chen Q, Yao Y, Yang W, et al. Verbal creativity correlates with the temporal variability of brain networks during the resting state. *Cereb Cortex.* 2019;29:1047–58. <https://doi.org/10.1093/cercor/bhy010>.
51. Christoff K, Irving ZC, Fox KCR, Spreng RN, Andrews-Hanna JR. Mind-wandering as spontaneous thought: a dynamic framework. *Nat Rev Neurosci.* 2016;17:718–31. <https://doi.org/10.1038/nrn.2016.113>.
52. Kaiser RH, Whitfield-Gabrieli S, Dillon DG, Goer F, Beltzer M, Minkel J, et al. Dynamic resting-state functional connectivity in major depression. *Neuropsychopharmacology.* 2016;41:1822–30. <https://doi.org/10.1038/npp.2015.352>.
53. Ruberto VL, Jha MK, Murrrough JW. Pharmacological treatments for patients with treatment-resistant depression. *Pharmaceuticals.* 2020;13:116. <https://doi.org/10.3390/ph13060116>.
54. Tozzi L, Zhang X, Pines A, Olmsted AM, Zhai ES, Anene ET, et al. Personalized brain circuit scores identify clinically distinct biotypes in depression and anxiety. *Nat Med.* 2024; 1–12. <https://doi.org/10.1038/s41591-024-03057-9>.
55. Imazu S, Ikeda S, Toi Y, Sano S, Kanazawa T, Shinosaki K, et al. Real-world outcome of rTMS treatment for depression within the Japanese public health insurance system: registry data from Kansai TMS network. *Asian J Psychiatry.* 2024;97:104082. <https://doi.org/10.1016/j.ajp.2024.104082>.
56. Taylor SF, Ho SS, Abagis T, Angstadt M, Maixner DF, Welsh RC, et al. Changes in brain connectivity during a sham-controlled, transcranial magnetic stimulation trial for depression. *J Affect Disord.* 2018;232:143–51. <https://doi.org/10.1016/j.jad.2018.02.019>.
57. Xia M, Liu J, Mechelli A, Sun X, Ma Q, Wang X, et al. Connectome gradient dysfunction in major depression and its association with gene expression profiles and treatment outcomes. *Mol Psychiatry.* 2022;27:1384–93. <https://doi.org/10.1038/s41380-022-01519-5>.
58. Hajdukka-Dér B, Kiss G, Sztahó D, Vicsi K, Simon L. The applicability of the beck depression inventory and hamilton depression scale in the automatic recognition of depression based on speech signal processing. *Front Psychiatry.* 2022;13. <https://doi.org/10.3389/fpsy.2022.879896>.
59. Moran PJ, Mohr DC. The validity of beck depression inventory and hamilton rating scale for depression items in the assessment of depression among patients with multiple sclerosis. *J Behav Med.* 2005;28:35–41. <https://doi.org/10.1007/s10865-005-2561-0>.
60. Schneibel R, Brakemeier E-L, Wilbertz G, Dykierok P, Zobel J, Schramm E. Sensitivity to detect change and the correlation of clinical factors with the hamilton depression rating scale and the beck depression inventory in depressed inpatients. *Psychiatry Res.* 2012;198:62–67. <https://doi.org/10.1016/j.psychres.2011.11.014>.
61. Seemüller F, Schennach R, Musil R, Obermeier M, Adli M, Bauer M, et al. A factor analytic comparison of three commonly used depression scales (HAM-D, MADRS, BDI) in a large sample of depressed inpatients. *BMC Psychiatry.* 2023;23:548. <https://doi.org/10.1186/s12888-023-05038-7>.
62. Brosch K, Stein F, Meller T, Schmitt S, Yuksel D, Ringwald KG, et al. DLPFC volume is a neural correlate of resilience in healthy high-risk individuals with both childhood maltreatment and familial risk for depression. *Psychol Med.* 2022;52:4139–45. <https://doi.org/10.1017/S0033291721001094>.
63. Steinbeis N, Bernhardt BC, Singer T. Impulse control and underlying functions of the left DLPFC mediate age-related and age-independent individual differences in strategic social behavior. *Neuron.* 2012;73:1040–51. <https://doi.org/10.1016/j.neuron.2011.12.027>.
64. Wang J, Wang Y, Hu Z, Li X. Transcranial direct current stimulation of the dorsolateral prefrontal cortex increased pain empathy. *Neuroscience.* 2014;281:202–7. <https://doi.org/10.1016/j.neuroscience.2014.09.044>.

ACKNOWLEDGEMENTS

We thank the members of the REST-meta-MDD consortium for their effort in the collection, organization, and sharing of their datasets. This work was supported by the STI 2030–Major Projects [grant number 2022ZD0208500-DY], Sichuan Science and Technology Program [grant number 2023NSFSC1185-XZ], Special Fund for Basic Scientific Research of Central Colleges [grant number ZYGX2021J036-KMK], and the Key R&D Program of Sichuan Province [grant number 2023YFS0076-TC]. Any opinions, findings, conclusions or recommendations expressed in this publication do not reflect the views of the Government of the Hong Kong Special Administrative Region or the Innovation and Technology Commission.

AUTHOR CONTRIBUTIONS

Conceptualization: QL, XZ, BB and WZ; Methodology: QL, XZ, BB and WZ; Formal Analysis: QL, XZ and WZ; Data curation: QL, XZ, CL, XX, YC, BZ, BB and WZ; Investigation: QL, XZ, CL, XX, YC, BZ, BB and WZ; Visualization: QL, XZ and CL; Supervision: BB and WZ; Funding acquisition: XZ, DY, KMK and TC; Writing – original draft: QL, XZ, BB and WZ; Writing – review & editing: QL, XZ, TC, JW, DY, KMK, BB and WZ.

COMPETING INTERESTS

The authors declare no competing interests.

ADDITIONAL INFORMATION

Supplementary information The online version contains supplementary material available at <https://doi.org/10.1038/s41398-025-03413-4>.

Correspondence and requests for materials should be addressed to Benjamin Becker or Weihua Zhao.

Reprints and permission information is available at <http://www.nature.com/reprints>

Publisher's note Springer Nature remains neutral with regard to jurisdictional claims in published maps and institutional affiliations.



Open Access This article is licensed under a Creative Commons Attribution-NonCommercial-NoDerivatives 4.0 International License, which permits any non-commercial use, sharing, distribution and reproduction in any medium or format, as long as you give appropriate credit to the original author(s) and the source, provide a link to the Creative Commons licence, and indicate if you modified the licensed material. You do not have permission under this licence to share adapted material derived from this article or parts of it. The images or other third party material in this article are included in the article's Creative Commons licence, unless indicated otherwise in a credit line to the material. If material is not included in the article's Creative Commons licence and your intended use is not permitted by statutory regulation or exceeds the permitted use, you will need to obtain permission directly from the copyright holder. To view a copy of this licence, visit <http://creativecommons.org/licenses/by-nc-nd/4.0/>.

© The Author(s) 2025